A Wavelet-Based Approach for Ultrasound Image Restoration

Mohammed Tarek GadAllah [1] and Samir Mohammed Badawy [2]

***Abstract* — Ultrasound's images are generally affected by speckle noise which is mainly due to the scattering phenomenon's coherent nature. Speckle filtration is accompanied with loss of diagnostic features. In this paper a modest new trial introduced to remove speckles while keeping the fine features of the tissue under diagnosis by enhancing image's edges; *via Curvelet denoising* and *Wavelet based image fusion*. Performance evaluation of our work is done by four quantitative measures: the *peak signal to noise ratio* (PSNR), the *square root of the mean square of error* (RMSE), a *universal image quality index* (Q), and the Pratt's *figure of merit* (FOM) as a quantitative measure for edge preservation. Plus Canny edge map which is extracted as a qualitative measure of edge preservation. The measurements of the proposed approach assured its qualitative and quantitative success into *image denoising while maintaining edges as possible.* A Gray phantom is designed to test our proposed enhancement method. The phantom results assure the *success and applicability of this paper approach* not only to this research works but also for *gray scale diagnostic scans' images* including ultrasound's B-scans.**

Keywords* — *Ultrasound Medical Imaging; Curvelet Based Image Denoising; Wavelet Based Image Fusion.

I. INTRODUCTION

Ultrasound medical imaging which has been widely accepted as an essential safe tool for biological tissue medical diagnosis, are generally affected by speckle noise due to the scattering phenomenon's coherent nature. Speckle noise is a well known phenomenon inherent most B-mode ultrasonic scans' images caused by the constructive and destructive interferences of the wavelets scattered by the tissue components as they arrive at the transducer [1], [2]. Speckle degrades the resolution and contrast of ultrasound images [3]. Speckle noise poses a well known problem in ultrasound imaging [4]. It acts as a mask of the small differences in grey level images [5]. Therefore the pre filtering process of Speckle noise cannot be avoided. It is a critical pre-processing step, providing clinicians with enhanced diagnostic ability [13]. The filtration is accompanied with loss of diagnostic features. The amount of these losses differs according to the techniques reported so far.

For example; the Multiscale Method introduced by *Achim, A. ... et al;* in [29]. The wavelet based denoising is one of the effective filtration techniques, like the technique introduced by *Pizurica, A. ... et al;* in [30], and the method introduced by *Rabbani, H. ... et al;* in [31]. Wavelets have been widely used in signal and image processing for the past 20 years [18], [19], [27], and [28]. Wavelet transform and its derivatives have many applications in biomedical image [1]processing [6]-[13] and [17]-[28]. The first introducing for wavelets into biomedical imaging research was in 1991; by *Weaver, J. B. ... et al,* in a journal paper [21] describing the application of wavelet transforms for noise reduction in MRI images, [19]. One of its derivatives is the *Curvelet Transform* (CVT) which first mentioned by E. J. Candµes and D. L. Donoho in 1999 [15]. The *Digital Curvelet Transform* (DCT) was introduced by D. L. Donoho & M. R. Duncan in *November* 1999 [16]. J.L. Starck, E.J. Candes, and D.L. Donoho published: "The Curvelet Transform for Image denoising" in 2002; [12]. Image denoising in Curvelet domain has enhanced denoising; due to the ability of *Curvelet Transform* to recover signals in different directions as compared with other methods [6]-[13]. Denoising in Curvelet domain has better results for speckle noise reduction of ultrasonic scans' images, but; in some cases *it cannot maintain all features of the scan's image*. This is a well-known problem in the field of biomedical imaging and image processing [32]-[40].

In this paper; we introduce an approach to remove speckles while keeping the fine features of the tissue under diagnosis as possible by enhancing image's edges; *via* the *Curvelet denoising* and *Wavelet based image fusion*. The study was done on a normal kidney ultrasonic scan taken from a man; 27 years old, by an ultrasound console: Aloka-ProSound 3500SX, in DICOM format [49]. Beside; an *original Gray phantom* is built to prove the success of our proposed enhancement method into better speckle reduction with edge enhancement for ultrasound scans, than the only Curvelet based denoising; qualitatively and quantitatively. A general quality optimization index S&M (S. Badawy and M. GadAllah) is newly introduced for selecting the best parameter's value for any parameter-based image fusion method being firstly introduced into image processing research. The paper is organized as follows: In Section II; we display the materials and methods had been used in our paper including our proposed approach, been applied on a human right kidney scan and the gray phantom study. The numerical and graphical results are displayed in Section III. A brief discussion of our results is represented in Section IV. Finally, we give some concluding remarks in Section V.

---

[1] **Mohammed Tarek GadAllah**; *is with* a company; as a *Maintenance & Operating Engineer, Broadcast Division,* at; Filka Television Broadcasting Station - Filka Island – Kuwait. (E-mail: **mohammed.tag.1986@gmail.com), (**Phone: **00965-97-466-049)**

[2] **Samir Mohammed Badawy;** *is a Doctor Emeritus with* the Faculty of Electronic Engineering, Menofia University, Menofia, Egypt. (E-mail: **drsamirb@gmail.com), (**Phone: **002-0100-8409-506)**

II. MATERIALS AND METHODS

A. Curvelet Based Image Denoising:

The Curvelets is to represent a curve as a superposition of functions of various lengths and widths [11]. Curvelet transforms gave close and improved delineation to edges [14]. Curvelet construction based on three essential ideas: firstly, *Ridgelets*; a method of analysis suitable for objects with discontinuities across straight lines. Secondly, *Multiscale Ridgelets*, a pyramid of windowed Ridgelets, renormalized and transported to a wide range of scales and locations. Thirdly, *Band-pass Filtering*, a method of separating an object out into a series of disjoint scales [15]. We used a Matlab-based Toolbox: [33] made by Sandeep P.; for performing *Image denoising in Curvelet domain using thresholding*. This toolbox [33]; when computing the Curvelet of an image, it makes that as given in [12].

B. Wavelet Based Image Fusion:

The principle of image fusion using wavelets is to merge the wavelet decompositions of the two original images using fusion methods applied to approximations coefficients and details coefficients [50]. There are more techniques for image fusion [41]-[44].

We used *the Wavelet toolbox, built-in Matlab-R2011b* to perform: *wavelet based image fusion;* a kind of a Multiscale-Decomposition Based Fusion. The fusion been made, was in-between the noisy image (**N**) and the reconstructed (denoised) image (**R**) produced from the denoising process in Curvelet transform domain. The resulted fused image, we called the final processed image (**FP**). An illustrative block diagram of the used fusion method is shown in **Fig.1**, *where;*

N is referred to the **N**oisy image -input.
R is referred to the **R**econstructed image -input.
A is referred to **A**pproximation.
D is referred to **D**etails.
FP is referred to **F**inal **P**rocessed image –output.

We applied the *User-Defined Fusion method*; mentioned in [50] for merging the approximation coefficients of the two input images; $\mathbf{A_N}$ and $\mathbf{A_R}$, as the following ***Matlab code***:

function A_{FP} *= my_fusion* (A_N, A_R)
D = true (size (A_N)*);* $F = 0.50$*;*
$A_{FP} = A_N$*;*
$A_{FP}(D) = F * A_N(D) + (1-F) * A_R(D)$*;*
$A_{FP}(\sim D) = F * A_R(\sim D) + (1-F) * A_N(\sim D)$*;*
end

The parameter **F**; we called the ***fusion ratio***; for the Approximation fusion method. The value of **F** can be changed from **0** to **1**. In our study we used different values of **F**. The best used value of **F** was **0.5;** achieving a maximum image's edge preservation as well as maintaining its quality as possible. **So,** we recommend using a value of **0.5** for **F**.

C. Performance Evaluation:

1) **RMSE** is the square root of **MSE** calculated from the following equation **(1):**

$$MSE = \frac{1}{m \times n} \sum_{i=1}^{m} \sum_{j=1}^{n} [\| O(i,j) - R(i,j) \|]^2 \quad \text{... (1)}$$

Where; **m** = number of rows in the image, **n** = number of columns, **O** is the original image pixel values matrix, **R** is the reconstructed image pixel values matrix, and finally **(i,j)** are the **x, y** coordinates for every pixel in each image. **MSE** has been the dominant quantitative performance metric in the field of signal processing for more than 50 years [45]. We had programmed; equation (1) of MSE, on *Matlab-R2011b* and implemented it in our measurements.

2) **PSNR** is represented in the following equation **(2):**

$$\text{PSNR} = 10 \log\left(\frac{MAX_O^2}{\text{MSE}}\right) \quad \text{... (2)}$$

Where, $\boldsymbol{MAX_o}$ is the maximum pixel value in image O [here; MAX_o = 255], MSE here is the mean square error calculated from equation (1). We used *Matlab-R2011b* and [33] for calculating PSNR. PSNR and RMSE measures are used in more papers which are about sonograms' denoising [11].

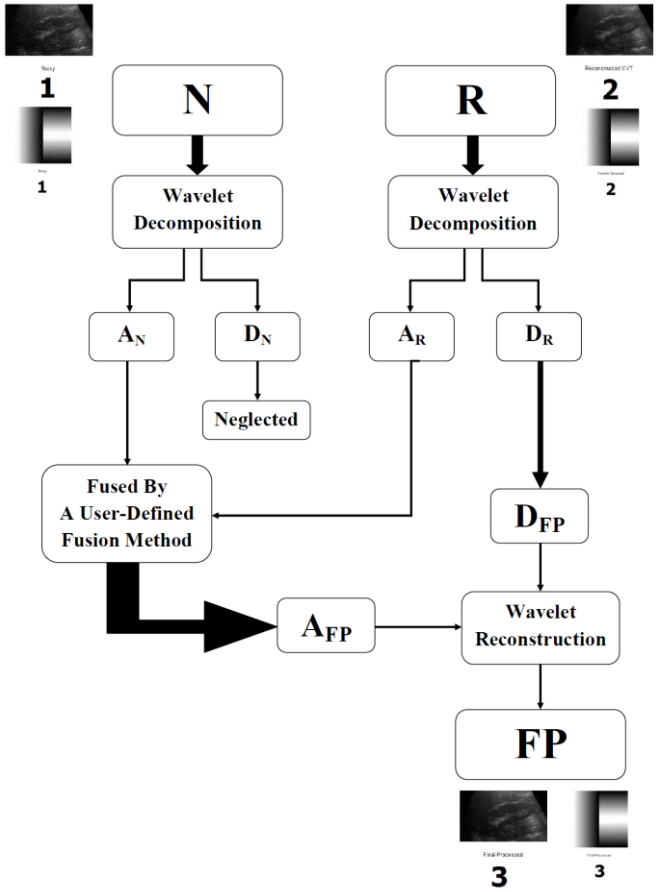

Fig. 1. Illustrative Block Diagram of the Used Fusion Method

3) **Q** is the Universal Image **Q**uality Index, introduced in [46], it is based on three basic components measured in-between the original image and the image which to be compared; correlation coefficient, mean luminance, and contrast [46]. Its value ranges from 0 till 1, if Q = 1, it means the two images are same. We used [46] and Matlab to calculate Q in our measurements.

4) **FOM** is the Pratt's **F**igure **o**f **M**erit; introduced in 1978 by W. K. Pratt as a quantitative measure for edge preservation [47]. FOM is defined by:

$$R = \frac{1}{\mathrm{I_N}} \sum_{i=1}^{I_A} \frac{1}{1 + \mathrm{a}D^2} \quad \dots \textbf{(3)}$$

Where; $\mathrm{I_N}$ = MAX $\{I_I, I_A\}$ and I_I and I_A represent the number of ideal and actual edge map points; *respectively*, *a* is a scaling constant, and *D* is the separation distance of an actual edge point normal to a line of ideal edge points. The rating factor is normalized so that $R = 1$ for a perfectly detected edge [47]. We used [48] by Matlab to calculate FOM in our measurements, but in *percent %* values, so if FOM = 100, it means that FOM = 1 in **(3).**

D. The Proposed Approach

An ultrasound scan of a normal human right kidney was taken by ultrasound console: *Aloka-ProSound 3500SX*; [49]. The interested area of the resulted image had been put on a black background with an appropriate dimensions match with Curvelet transform domain; as shown in **Fig.2.**

Manipulation was done as follow:

i. Noising the image by an added noise determined by the value of the Signal to Noise Ratio **(Snr).**
ii. Denoising the resulted image in Curvelet transform domain, as mentioned previously in **A.**
iii. Applying the wavelet based fusion method been explained previously in **B.**; in-between the noised and the denoised image produced from **i.** and **ii.**, respectively taking **F = 0.95959595.**
iv. *Measurements:*
   - The edge detection map of Canny had been extracted as a qualitative measure of edge preservation for each image of the three images produced from **i., ii.,** and **iii.**
   - A four quantitative performance evaluation measures PSNR, RMSE, Q, and FOM; had been calculated in-between the original image and each one of its three derivatives produced in **i., ii.,** and **iii.**
v. Repeating the previous four steps **i., ii., iii.,** and **iv.;** along **20** different values for Snr.
vi. The FOM's **20** results is plotted for each image vs. the corresponding Snr, into **Fig.3-A,** where: the three colored lines; Blue, Green, and Red represents: in the three cases: Noisy, denoised (CVT), and the final wavelet fused image (WT), respectively.

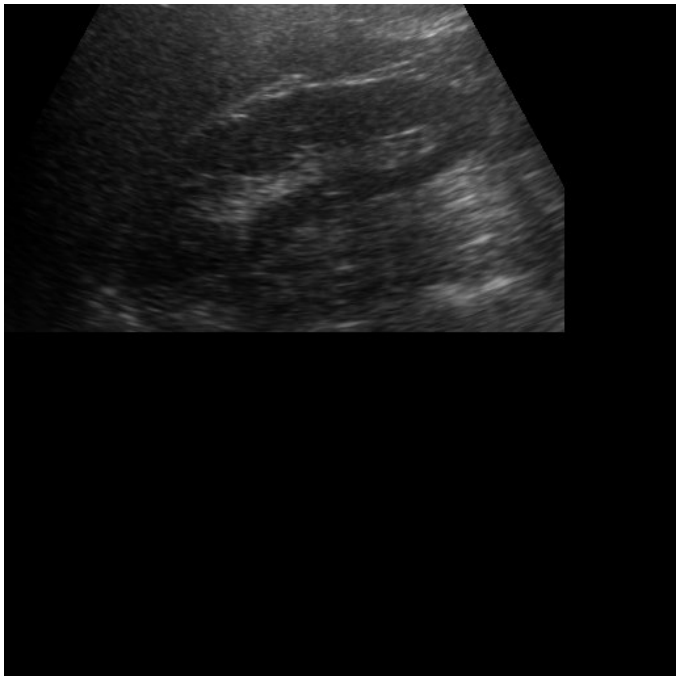

Fig. 2. The Right Kidney Scan On A Black Background

Optimizing the Applied Fusion Method:

Our goal is to find the better performance of the applied fusion method that makes maximum edge preservation as well as maintains image's quality and PSNR as possible. For that we introduce here, a general quality optimization index be named S&M index. This index can be used in general for selecting the best parameter's value *(**F** in our study)* for any parameter-based image fusion method being firstly introduced into image processing research. S&M index is defined as follow:

$$S\,\&\,M = \frac{\%\mathrm{PSNR\_n} \times \%\mathrm{FOM\_n} \times \%\mathrm{Q\_n}}{\%\mathrm{RMSE\_n} \times 100}\,\% \quad \dots \textbf{(4)}$$

Where, **_n**: means after normalization to the nearest maximum value. This equation calculates maximum values for PSNR, FOM, Q, and minimum value for RMSE.

We applied S&M optimization for the applied fusion method as follow:

1) *Taking* one result from the right kidney scan's image, where Snr = 10, after step **ii;** i.e. after noising and denoising process, then, we made step iii for this result not only at (F) = 0.95959595, But, instead we made this step **25** times for different values of **F**; starting from **0.05** to **1.0.**

2) Calculating the four measurements; PSNR, RMSE, Q, and FOM; for all the 25 results, and normalized all to the nearest maximum value.

3) Drawing in percentage %; the 25 final wavelet fused numerical results for PSNR, RMSE, Q, and FOM, after being approximately normalized; all vs. the fusion ratio (**F**); as

shown in **Fig.3-B;** where: the four colored lines; Blue, Green, Red, and Blue-Light represents: the four measurements: PSNR, RMSE, Q, and FOM; respectively.

4) Finally, we applied equation (4), for S&M optimization index, on the 25 results from the previous step **2**, producing the optimization figure; shown in **Fig.3-C;** where: the y-axis; represents: S&M index value, and the x-axis; represents: **F**; starting from **0.05** to **1.0.**

Repeating Manipulation taking F = 0.5:

From equation (**4**); we can deduce that the optimum performance of the proposed approach, *making maximum edge preservation as well as maintaining image's quality and PSNR as possible;* can be founded where S&M index has a maximum value. From **Fig.3-C;** the maximum value of S&M index on the curve can be founded when **F = 0.5.** Taking F = 0.5 instead of the last empirical value of F (0.95959595) and repeating our proposed approach's manipulation steps on the same image shown in **Fig. 2**, we will obtain another 20 optimized results. The FOM's measurement values during the 20 results are plotted into **Fig.3-D;** where*:* the three colored lines; Blue, Green, and Red represents: in the three cases: Noisy, CVT, and WT; respectively.

E. Our Gray Phantom Study:

A new Gray phantom shown in **Fig. 4;** been introduced by *S. Badawy and M. GadAllah;* consists of gray scale vertical and horizontal bars used for testing strait boundaries and intensities of the gray levels. It is designed especially to test and assure the applied method for all gray scale images in radiology including Ultrasound's B-Scans.

Processing steps:

a. Noising the phantom by an added noise determined by the **Snr** value.
b. Denoising the produced image in Curvelet transform domain.
c. Applying the wavelet based fusion method been explained previously in **B.**; in-between the noised and the denoised image produced from **a.** and **b.**, respectively taking **F = 0. 5**.
d. *Measurements:*
   - The edge detection map of Canny had been extracted as a qualitative measure of edge preservation for each image of the three images produced from **a., b.,** and **c.**
   - A four quantitative performance evaluation measures PSNR, RMSE, Q, and FOM; had been calculated in-between the original phantom image and each one of its three derivatives produced in **a., b.,** and **c.**
e. Repeating the previous four steps **a., b., c.,** and **d.;** along **12** different values for Snr.

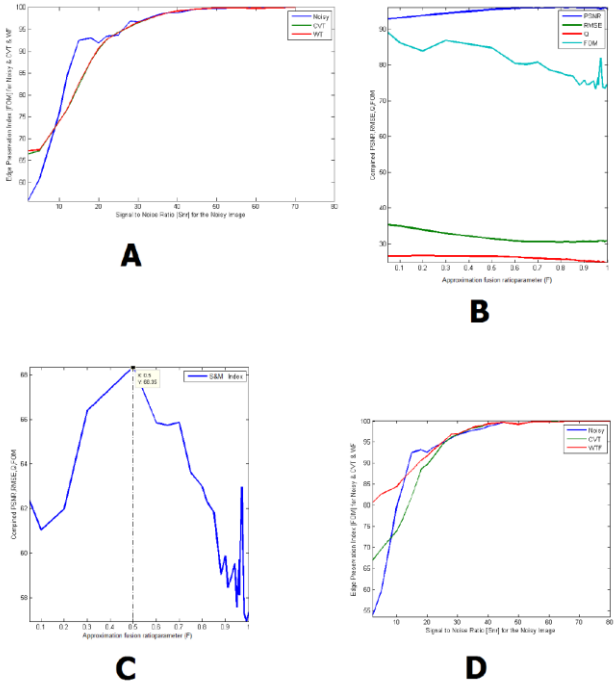

Fig. 3. Right Kidney Scan Image's Analytical Results Curves

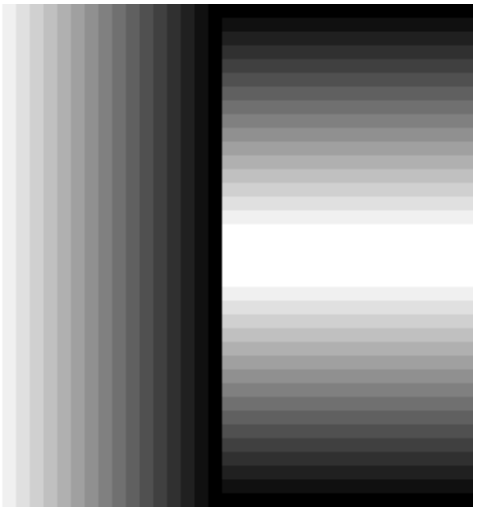

Fig. 4. Our New Gray Phantom

TABLE I. THE RIGHT KIDNEY SCAN AVERAGE RESULTS

Average Results for: **Final Wavelet Fused Image**	Final Output Before S&M Index Optimization	Final Output After S&M Index Optimization
Peak Signal to Noise Ratio [PSNR]	**56.39**	**56.29**
Mean Square of Error [MSE]	**3.45**	**3.87**
Root Mean Square of Error [RMSE]	**1.26**	**1.31**
Universal Quality Index [Q]	**0.34**	**0.34**
Edge Preservation Index [Pratt's FOM]	**91.04**	**94.09**

III. RESULTS

A. Kidney scan image Results with F = 0.95959595:

After applying our proposed approach on the right kidney scan's image, where; F = 0.95959595, and along 20 different value of Snr; the result is 20 by 3 images produced 60 resulted images beside the original one. After Canny edge map had been extracted producing another 60 result edge maps for each image beside the edge map of the original one.

The results was good but after being optimized; it became better; so, we satisfied here only by displaying the final average quantitative results of the 20 different results for: PSNR, RMSE, Q, and FOM, in comparison by the same average results after being optimized by the suitable fusion ratio based on applying S&M index enhancement, see **Table I.** Analytically; the FOM's 20 results had been plotted vs. the corresponding Snr, as shown in **Fig.3-A**.

B. Kidney scan image Results with F = 0.5:

After applying the S&M optimization on the right kidney scan's image, selecting (F) = 0. 5, and along 20 different value of Snr; the result is 20 by 3 images produced 60 resulted images beside the original one. After Canny edge map had been extracted producing another 60 result edge maps for each image beside the edge map of the original one. A sample result from the 20 results, *where Snr = 10*; can be seen in **Fig. 5;** *where:* The lower four images in the two figures are the *canny edge map* for the upper four images correspondingly. Those maps are a qualitative measure for edge preservation in each image. The numbers on images are as follow:

1) Is stated for the Noisy-Image.
2) Is stated for the Reconstructed –Image after the denoising process in Curvelet transform domain.
3) Is stated for the Final Processed - Image after making the wavelet based image fusion in between 1 & 2.
4) Is stated for the Original Base Image as a reference.

The final average quantitative results of the 20 different results for: PSNR, RMSE, Q, and FOM, after being optimized by the suitable fusion ratio; are shown in Table I. The FOM's 20 results had been plotted vs. the corresponding Snr, as shown in **Fig.3-D.**

C. Our Phantom Study Results:

Applying our enhancement approach on the gray scale phantom image, selecting (F) = 0. 5, and along 12 different value of Snr; the result is 12 by 3 images produced 36 resulted images beside the original one. After Canny edge map had been extracted producing another 36 result edge maps for each image beside the edge map of the original one. According to the tabulated results into **Table II;** we have up to twelve figures. A sample Result of our Gray Scale Phantom is shown in **Fig.6;** *Where;* Snr = 25 for the noisy image. *Where:* The lower three images are the *canny edge maps* for the upper three images correspondingly.

This is a qualitative measure for edge preservation in each image. The numbers on images are as follow:

1) Is stated for the Noisy-Image.
2) Is stated for the Reconstructed –Image after the denoising process in **C**urvelet **T**ransform (**CT**) domain.
3) Is stated for the Final Processed - Image after making the wavelet based image fusion in between 1 & 2.

The quantitative measurements taken from processing our Gray Phantom image had been tabulated into Table II; representing 12 Results' measurements, taking F_ratio = 0.5. Table II has equal number of elements. Each row describes one complete result measurements for a specified **S**ignal to **N**oise **R**atio (SNR) value taken for the noised image. The last row is the mean or **Avg. (**Average**)** values of each parameter. The first-left column represent the value of SNR, the next column is the result number, the next 8 columns are the measurements values, *Where*;

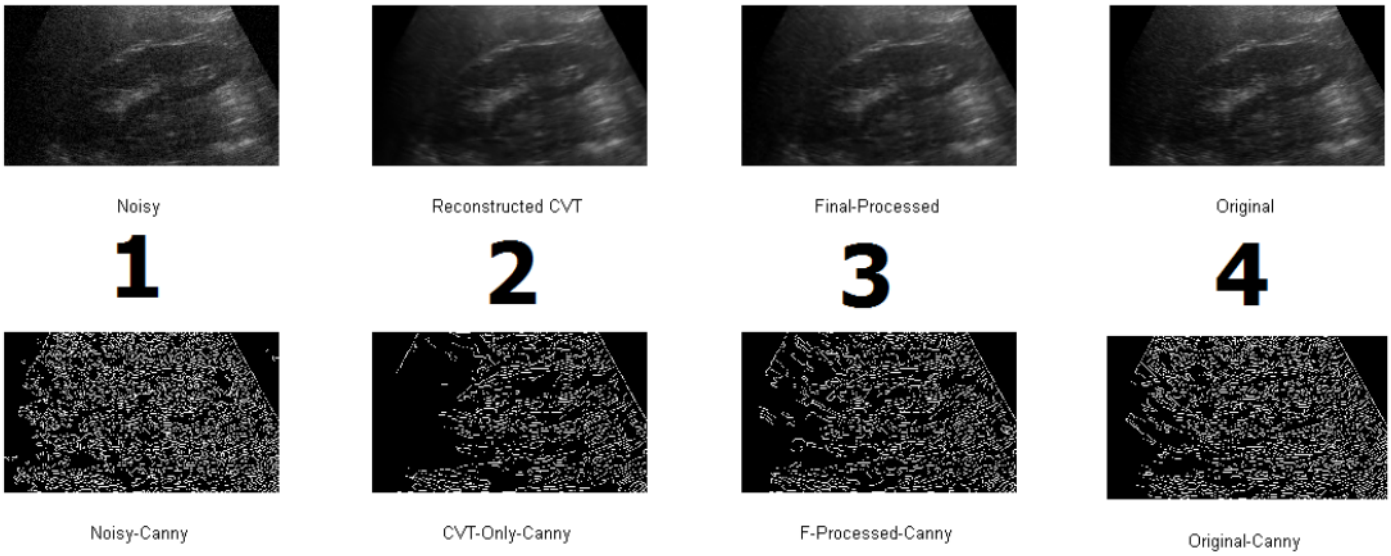

Fig. 5. A Sample Result for the Right Kidney Scan After Using **S&M** Index at Fusion Ratio, **F = 0.5,** *Where;* **Snr = 10**

Noisy - Snr: is the noisy image's *signal to noise ratio*.

Result - No.: is the *number of result*

Parameter + N: *N* refers to *Noisy* and means that this parameter is calculated in-between the noisy image and the reference original one shown in Fig.3.

Parameter + FP: *FP refers to **F**inal **P**rocessed by the applied approach,* and means that this parameter is calculated in-between the *Final Result wavelet-fused image* and the reference original one.

The four calculated measures' 12 results; *PSNR, RMSE, Q, and FOM;* had been plotted for each image *vs.* the corresponding Snr; producing four curves shown in **Fig.7:** A, B, C, and D respectively. *Where:* The Blue line represents the quantity before applying the processing approach (Noisy) and the Green line represents the same quantity after image being processed (FP).

IV. DISCUSSION

Looking at **Fig.3-A** & **Fig.3-D,** *obviously; we can see the enhancement in* the edge preservation index FOM for the final fused kidney scan image, *before and after applying S&M-optimization;* represented by the red line.

Quantitatively, Looking at **Table I,** we can notice the increase in FOM after the optimization process, where the value of Q is still constant; a*ssuring our optimized approach in preserving edges while maintaining quality as possible.*

Qualitatively; comparing in between the Canny edge map for the final fused images shown in **Fig.5-3**, and the denoised image using Curvelet only shown **in Fig.5-2;** we can see the effect of our proposed approach in recovering image details which lost in denoising process. *Comparing* in between the Canny edge map for the final processed image shown in **Fig.5-3,** and the noisy image shown in **Fig.5-1;** we can see the enhanced denoising produced while keeping edges as possible.

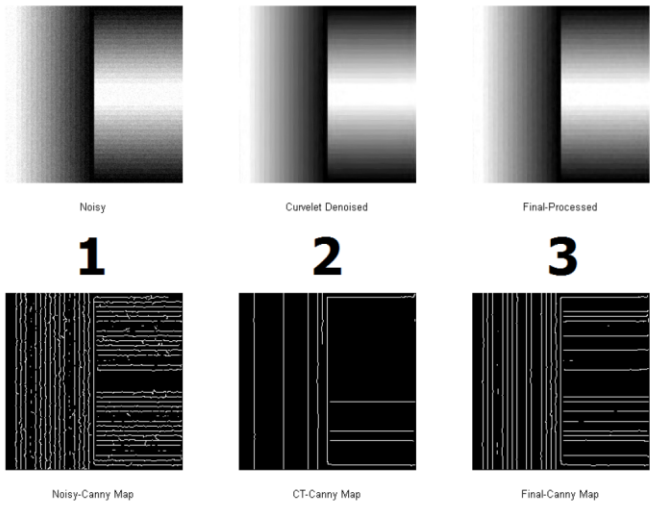

Fig. 6. A Sample Result of Our Gray Scale Phantom *Where;* **Snr = 25**

TABLE II. THE GRAY SCALE PHANTOM IMAGE'S RESULTS, *WHERE*; **F = 0. 5**

Noisy SNR	Result NO.	PSNR		RMSE		Q		FOM	
		N	FP	N	FP	N	FP	N	FP
2	1	6.07	22.53	126.81	19.06	0.01	0.19	35.34	49.29
5	2	9.07	25.29	89.78	13.86	0.02	0.28	35.35	51.14
8	3	12.07	27.76	63.56	10.44	0.03	0.38	36.95	57.22
10	4	14.07	29.36	50.49	8.68	0.05	0.45	37.83	60.13
12	5	16.07	30.71	40.10	7.44	0.07	0.52	39.07	67.97
15	6	19.07	32.44	28.39	6.09	0.11	0.60	43.91	76.58
18	7	22.07	34.04	20.10	5.06	0.19	0.67	55.46	69.92
20	8	24.07	35.15	15.97	4.46	0.26	0.72	61.81	80.68
25	9	29.07	38.23	8.98	3.13	0.50	0.81	87.24	78.58
30	10	34.07	43.20	5.05	1.76	0.72	0.89	93.51	75.97
40	11	44.07	49.62	1.60	0.84	0.89	0.91	93.97	97.11
50	12	54.07	57.61	0.50	0.34	0.91	0.91	100	100
Average		23.65	35.50	37.61	6.76	0.31	0.61	60.04	72.05

Looking at **Fig.7-A, Fig.7-B,** and **Fig.7-C;** for PSNR, Q, and FOM, *respectively*; we can see *analytically* the resulted enhancement in the final processed *gray scale image after applying our enhancement procedure;* represented by the green line instead of the blue line before enhancement. Also, RMSE had been decreased throw all the curve shown in **Fig.7-D;** represented by the green line instead of the blue line before.

Comparing in between the Canny edge map for the final fused phantom image shown in **Fig.6-3,** and the denoised image using Curvelet only shown in **Fig.6-2;** we can obviously; see the effect of our proposed approach in recovering some of image's details which lost in denoising process.

Comparing in between the Canny edge map for the final fused phantom image shown in **Fig.6-3,** and the noisy image shown in **Fig.6-1;** we can see *qualitatively*; the enhanced denoising produced by our proposed enhancement approach while keeping edges as possible preservation.

A clear improvement in the *average* value for FOM and Q can be shown *quantitatively* in **Table II;** to be **72.05** and **0.61** instead of **60.04** and **0.31**, *respectively*.

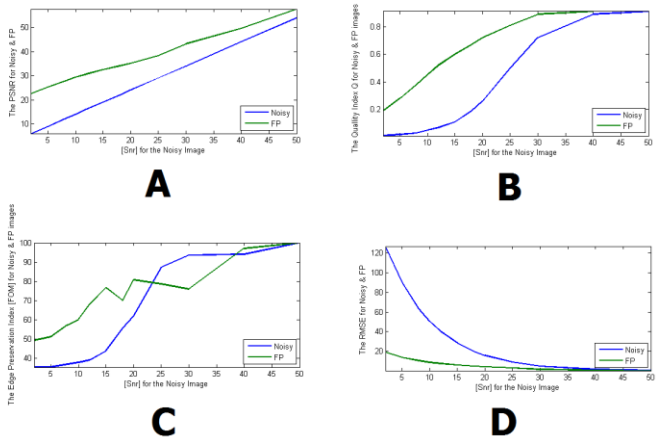

Fig. 7. Gray Scale Phantom Image's Analytical Results Curves

Also, the *average* value of PSNR was better enhanced after applying our probosed wavelet based approach to be **35.50** instead of **23.65** before.

On the other hand the *average* value of RMSE had been decreased to be **6.76** instead of **37.61** before; which assures that the applied approach is effective in *enhanced denoising with little values of error.*

The gray phantom results displayed is a step towards generalizing our introduced enhancement method for all gray scale diagnostic scans' images including Ultrasonography.

V. CONCLUSION

Wavelet based image fusion after Curvelet denoising, successfully used to *improve the removal of image's speckles* (*here,* kidney's ultrasound scan) while *enhancing its edges as possible.* Moreover, a gray phantom was introduced to help in testing and assuring the ability of the proposed work as an enhancement method for gray scale diagnostic scans' images including Ultrasonography. Also; a general quality optimization index be named S&M is newly introduced for selecting the best parameter for any parameter-based image fusion method being firstly introduced into image processing research.

ACKNOWLEDGMENT

Thanks to Dr. Mohammad Bahaa, *Consultant Radiologist,* Radiology Department, Specialized Clinic Center [SCC], Hawally, Kuwait; for his participation in the Practical work.

REFERENCES

[1] Andrew G. Webb, "Ultrasonic Imaging", Ch. (3), in *Introduction to Biomedical Imaging*, © 2003 IEEE, Inc., IEEE Press Series on Biomedical Engineering, pp. 107-153, Published by: John Wiley & Sons, Inc., Hoboken, New Jersey ISBN: 0-471-23766-3

[2] Shung, K. Kirk, "Gray-Scale Ultrasonic Imaging", Ch. 4, pp. 79-101, in *Diagnostic Ultrasound: Imaging and Blood Flow Measurements,* CRC Press, © 2006 by Taylor & Francis Group, LLC.

[3] Torbørn Eltoft, "Modeling the Amplitude Statistics of Ultrasonic Images", IEEE T Med Imaging, Vol. 25, No. 2, Feb. 2006

[4] K. Shahnazi and M. Fox, "Speckle Reduction in Real Time Ultrasound Imaging", © 1994 IEEE

[5] Christoph B. Burckhardt, "Speckle in Ultrasound B-Mode Scans", IEEE Transactions on Sonics and Ultrasonics, Vol. SU-25, No. 1, Jan. 1978, © 1978 IEEE

[6] Samir M. Badawy, Mohammed T. GadAllah and Mohammed M. Sharaf, "Intraocular Ultrasound Scan Examination by Image Segmentation", Mitteilungen Klosterneuburg, ISSN: 0007-5922, Volume: (64), Issue: (3), pp. 278-285, March 2014. URL: http://mitt-klosterneuburg.com/show.php?v=64&i=3

[7] Mohammed T. GadAllah, M. M. Sharaf, Fahima A. Essawy and Samir M. Badawy, "Visual Improvement for Hepatic Abscess Sonogram by Segmentation after Curvelet Denoising", *International Journal of Image, Graphics and Signal Processing* (IJIGSP), vol.5, no.7, pp.9-17, *DOI: 10.5815/ijigsp.2013.07.02,* June 2013. URL: http://www.mecs-press.org/ijigsp/ijigsp-v5-n7/IJIGSP-V5-N7-2.pdf

[8] Mohamed Tarek GadAllah & Samir Badawy, "Diagnosis of Fetal Heart Congenital Anomalies by Ultrasound Echocardiography Image Segmentation after Denoising in Curvelet Transform Domain", *Online Journal on Electronics and Electrical Engineering (OJEEE)*, ISSN (2090-0279), *Vol. (5), No. (2)*, pp. 554 - 560, *Ref. No. : W13-E-0023*, April 2013. URL: http://infomesr.org/attachments/W13-E-0023.pdf

[9] Mohamed T. GadAllah & Samir Badawy, "Aorta's abnormalities detection by Ultrasonography scan Denoising in Curvelet Transform Domain", Journal of Al-Azhar University Engineering Sector, JAUES, Vol. (7), No. (3), pp. 395 – 403, E38, Dec. 2012. *EJAUES website:* https://sites.google.com/site/ejaues

[10] H. Lazrag, M. Ali H., and M. Saber N., "Despeckling of Intravascular Ultrasound Images using Curvelet Transform", *SETIT*, March 2012.

[11] F. Y. Rizi, H. A. Noubari, and S. K. Setarehdan, "Wavelet-Based Ultrasound Image Denoising: Performance Analysis and Comparison", 33rd Conf. IEEE-EMBS, Boston, ©2011 IEEE

[12] J. Starck, E. J. Candès, and D. L. Donoho, "The Curvelet Transform for Image Denoising", IEEE Transactions on Image Processing, Vol. 11, No. 6, June 2002, pp. 670-684, © 2002 IEEE

[13] F. Yousefi Rizi, and S. K. Setarehdan, "Noise Reduction in Intravascular Ultrasound Images Using Curvelet Transform and Adaptive Complex Diffusion Filter: a Comparative Study", ICEE2012, Iran, 2012

[14] M. Elhabiby … et al, "Second Generation Curvelet Transforms Vs Wavelet transforms and Canny Edge Detector for Edge Detection from WorldView-2 data", *IJCSES, Vol.3, No.4,* Aug. 2012

[15] E. J. Candµes and D. L. Donoho, "Curvelets - A Surprisingly Effective Nonadaptive Representation for Objects with Edges", Saint-Malo Proceedings, Vanderbilt University Press, Nashville, TN, 1999, *Available:* http://www-stat.stanford.edu/~donoho/Reports/1999/curveletsurprise.pdf

Another URL: www.dtic.mil/cgi-bin/GetTRDoc?AD=ADP011978

[16] David L. Donoho and Mark R. Duncan, "Digital Curvelet Transform: Strategy, Implementation and Experiments", Technical Report No. 2000-12, Department of Statistics, Stanford University, March, 2000. *Available:* http://statweb.stanford.edu/~ckirby/techreports/GEN/2000/2000-12.pdf

[17] K. Ding, "Wavelets, Curvelets and Wave Atoms for Image Denoising", *3rd International CISP2010*, ©2010 IEEE

[18] Unser, M., Aldroubi, A., and Laine, A., "Guest Editorial: Wavelets in Medical Imaging", *Special issue,* IEEE Transactions on Medical Imaging, Vol. 22, No. 3, pp. 285-288, March 2003

[19] Y. Jin, E. Angelini, and A. Laine, "Wavelets in Medical Image Processing: Denoising, Segmentation, and Registration", Ch. 6, pp. 305-358, in *Handbook of Biomedical Image Analysis, Volume I: Segmentation Models Part A, By: J. S. Suri, D. L. Wilson, and S. L.,* © 2005 Kluwer Academic / Plenum Publishers, New York

[20] R. C. Gonzalez, R. E. Woods, "Wavelets and Multiresolution Processing", Ch. 7 pp. 349-408, *in Digital Image Processing, 2nd Ed.,* © 2002 *by Prentice-Hall, Inc., New Jersey 07458*

[21] Weaver, J. B. … et al, "Filtering noise from images with wavelet transforms", Magn. Reson. Med., Vol. 21, No. 2, pp. 288–295, 1991

[22] A. Achim, A. Bezerianos, and P. Tsakalides, "Ultrasound Image Denoising Via Maximum A Posteriori Estimation of Wavelet Coefficients", *Proceedings of the 23rd Annual International Conference of the* IEEE-EMBS, Vol. 3, pp. 2553–2556, 2001

[23] M. Misiti, Y. Misiti, G. Oppenheim, and J. Poggi, "Image Processing with Wavelets", Ch. 8, pp. 235-276, and, "An Overview of Applications", Ch. 9, pp. 279-310, in *Wavelets and their Applications*, © ISTE Ltd, London W1T 5DX, UK, 2007

[24] James S. Walker, "Wavelet-Based Image Processing, *To Berlina*", Applicable Analysis, Vol. 85, No. 4, 2006, pp. 439-458, *Available:* http://www.uwec.edu/walkerjs/media/WBIP.pdf

[25] Øyvind Ryan, "Applications of the wavelet transform in image processing", Dep. of informatics, University of Oslo, 12 Nov. 2004

[26] Adhemar Bultheel, "Wavelets with Applications in Signal and Image processing", Oct. 25, 2002, *Available:* http://f3.tiera.ru/ShiZ/math/Signals/Bultheel/Wavelets%20with%20Applications.pdf

[27] R. Polikar, "The Story of Wavelets", © IMACS/IEEE CSCC'99 Proceedings, pp.5481-5486, 1999

[28] M. Unser, and A. Aldroubi, "A Review of Wavelets in Biomedical Applications", Invited Paper, Proceedings of the IEEE, Vol. 84, No. 4, April 1996, pp. 626-638, © 1996 IEEE

[29] A. Achim, A. Bezerianos, and P. Tsakalides, "Novel Bayesian Multiscale Method for Speckle Removal in Medical Ultrasound Images", *IEEE*

Transactions on Medical Imaging, Vol. 20, No. 8, pp. 772–783, Aug. 2001

[30] A. Pizurica, W. Philips, I. Lemahieu, and M. Acheroy, "A Versatile Wavelet Domain Noise Filtration Technique for Medical Imaging", *IEEE Transactions on Medical Imaging*, Vol. 22, No. 3, pp. 323–331, March 2003

[31] H. Rabbani … et al, "Speckle Noise Reduction of Medical Ultrasound Images in Complex Wavelet Domain Using Mixture Priors", IEEE-TBME, Vol. 55, No. 9, Sep. 2008, ©2008 IEEE

[32] Mohamed Ali Hamdi, "A Comparative Study in Wavelets, Curvelets and Contourlets as Denoising Biomedical Images", I.J. Image, Graphics and Signal Processing, 2012, 1, pp. 44-50, © 2012 MECS

[33] Sandeep Palakkal, "Ridgelet and Curvelet first generation Toolbox", 25 May 2011, (Updated 21 Mar 2012), http://www.mathworks.com/matlabcentral/fileexchange/31559-ridgelet-and-curvelet-first-generation-toolbox

[34] Anil A. Patil, and J. Singhai, "Image denoising using curvelet transform: an approach for edge preservation", Journal of Scientific & Industrial Research, Vol. 69, pp. 34-38, Jan. 2010

[35] Tamilselvi, P.R., and P. T., "Noise suppression and improved edge texture analysis in kidney ultrasound images", ICICT- 2010

[36] Ahmed Badawi, "Scatterer Density in Nonlinear Diffusion for Speckle Reduction in Ultrasound Imaging: The Isotropic Case ", *World Academy of Science, Engineering and Tech., 13,* 2008

[37] Z. Yang, and M. D. Fox, "Speckle Reduction and Structure Enhancement by Multichannel Median Boosted Anisotropic Diffusion", *EURASIP Journal on Applied Signal Processing 2004:16*, pp. 2492–2502, © 2004 Hindawi Publishing Corporation

[38] K. Z. Abd-Elmoniem, A. M. Youssef, and Y. M. Kadah, "Real-Time Speckle Reduction and Coherence Enhancement in Ultrasound Imaging via Nonlinear Anisotropic Diffusion", *IEEE-TBME*, Vol. 49, No. 9, pp. 997-1014, Sep. 2002, ©2002 IEEE

[39] X. Zong … et al, "Speckle Reduction and Contrast Enhancement of Echocardiograms via Multiscale Nonlinear Processing", IEEE Transactions on Medical Imaging, Vol. 17, No. 4, pp.532-540, 1998

[40] Richard N. C., Douglas L. Jones, and W. D. O'Brien, "Ultrasound Speckle Reduction by Directional Median Filtering", © 1995 IEEE

[41] R. Blum, Z. Xue, and Z. Zhang, "An overview of image fusion," Ch. 1, in *Multi-Sensor Image Fusion and Its Applications,* pp. 1–36, CRC Press Taylor and Francis Group, 2006

[42] Paul M. de Zeeuw … et al, "Multimodality and Multiresolution Image Fusion", *VISAPP* 2012, pp. 151-157

[43] Paul M. de Zeeuw, "A Multigrid Approach to Image Processing", *R. Kimmel, N. Sochen, J. Weickert (Eds.): Scale-Space 2005,* LNCS 3459, pp. 396–407, 2005, © Springer-Verlag Berlin Heidelberg

[44] Hui Li, B. S. Manjunath, and S. K. Mitra, "Multi-Sensor Image Fusion Using the Wavelet Transform", ©1994 IEEE

[45] Zhou Wang and Alan C. Bovik, "Mean Squared Error: Love It or Leave It? *A New Look at Signal Fidelity Measures*", IEEE Signal Processing Magazine, Vol. 26, No. 1, pp. 98-117, Jan. 2009.

[46] Zhou Wang, "Free Matlab based software program for calculating the Universal Image Quality Index; Q", Copyright (c) 2001 The University of Texas at Austin, *Available:* http://www.cns.nyu.edu/~zwang/files/research/quality_index/img_qi.m

The original source paper is: Zhou Wang, and Alan C. Bovik, "A Universal Image Quality Index", *Signal Processing Letters, IEEE,* ISSN: 1070-9908, Vol. 9, Issue: 3, pp. 81-84, DOI: 10.1109/97.995823, March 2002

[47] W. K. Pratt, "Edge Detection", Ch. 15, pp. 443-508, *in Digital Image Processing: PIKS Inside, 3rd Ed., by William K. Pratt,* ISBN: 0-471-22132-5, © 2001 by John Wiley & Sons, Inc.

[48] Bjency, "*matlab source code for* Edge preservation measure Index: Pratt's Figure of Merit", Programmers United Develop Net [PUDN], 23 Oct. 2009, *Website:* http://en.pudn.com/downloads201/sourcecode/graph/texture_mapping/detail947301_en.html

[49] Ultrasound Console: ProSound 3500SX, Hitachi Aloka Medical, Ltd., *URL:* http://www.aloka.com/products/view_system.asp?id=3

[50] Fusion of two images, image analysis, discrete wavelet analysis, Wavelet Toolbox, Documentation Center, MathWorks website, URL: http://www.mathworks.com/help/wavelet/ref/wfusimg.html

AUTHORS PROFILE

Mohammed Tarek GadAllah was born in Menofia, Egypt on December-29th 1986. He is *now* working with a company; as a *Maintenance & Operating Engineer, Broadcast Division,* at; Filka Television Broadcasting Station - Filka Island – Kuwait. He is *engineer on leave* from *El Nasr Electric And Electronic Apparatus Co.* [NEEASAE], Alexandria, Egypt. Mohammed was awarded the Degree of Bachelor of Electronic Engineering in July 29th, 2008 from *Industrial Electronics and Control Engineering Department,* Faculty of Electronic Engineering, Menofia University - Menofia, Egypt. Mohammed now has more than one achievement in designing and fabricating electronic circuits. Mohammed is now a *post-graduate – master student* at *Industrial Electronics and Control Engineering Department,* Faculty of Electronic Engineering, Menofia University, Egypt. Mohammed, *as well as this paper*, has four published papers: **[6], [7], [8],** and **[9].** His *previous and current research interests include:* Biomedical Image Processing, Biomedical Engineering, Medical Imaging, Digital Control, and Electronic Circuits.

Samir Mohammed Badawy is now a *Doctor Emeritus, Department of Industrial Electronics and Control Engineering,* Faculty of Electronic Engineering, Menofia University - Menofia, Egypt. Samir had received his Ph.D. degree from Institute of cancer research, Royal Marsden Hospital, London University, UK. He had received his Master Degree from Helwaan University, Egypt. He was awarded the Degree of Bachelor of Engineering from *Industrial Electronics Department,* Faculty of Engineering, Menofia University – Egypt. His *previous and current researches interests include:* Biomedical Physics, Biomedical Electronic, BCI, ECI, Medical Image Processing, Enhancement and Analysis, Ultrasound Tissue Characterization and Reconstruction, and biological Magnetic Effects on living cells.